

# Implementation on Image Compression and Using Vector Quantization and Other Efficient Algorithms

Mr. Surya Pratap Singh<sup>1\*</sup> Dr. Bharti Chourasia<sup>2</sup>

<sup>1</sup> Research Scholar, SRK University, Bhopal

<sup>2</sup> Head EC Department, SRK University Bhopal

**Abstract – For all the purposes, capable, cross breed coding compression frameworks have now been developed, which consolidate the advantages of different traditional image coding techniques. Exploratory findings demonstrate that the current compression plans will de-associate knowledge dependency in both the space and the space areas in a constructive and sufficient way. The best basic compression ratio as compared and the newest lossless Bayer compression plans are then offered. The Lossy compression image plans are repeated in the same rate as the new SSACI compression strategy, using improved visual clarity, less impeding antiques and better PSNR.**

**Keywords – Image Compression, Vector Quantization, Digital Communication, Sensors etc.**

-----X-----

## I. INTRODUCTION

The encoding of images addresses the issue of reducing the number of data required for a digital file. It is a process designed to produce a compact image representation that reduces the transmission requirements for image storage. Each picture has information that is redundant. Redundancy is the reproduction of the image data. Image compression occurs through the use of redundant information in the image. The image is often reproduced, but the image is compressed more frequently. Redundancy reduction contributes to the storage of image space. Photo compression is carried out when one or more of these redundancies are minimized or eliminated. In the compression of images, three simple data redundancies can be established and manipulated. Failure to release one or more of the three fundamental data contributes to compression [1].

### a) Inter Pixel Redundancy

The pixels next to the picture, statistically speaking, are not independent. It is responsible for the similarity in the picture with the pixels nearby. This redundancy is regarded as redundancy inter-pixel. This kind of redundancy is often named spatial redundancy, too. By having a pixel value dependent on its adjacent pixel values, this redundancy may be explored in a variety of ways. The initial 2-D pixel array is typically mapped to another format for this reason, such as an array of variations between neighboring pixels. Mapping is claimed to be reversible if the transformed data set

can restore the original pixel[3] image. Identify the sponsor(s) in the discussion [3].

### b) Coding Redundancy

This includes the use of variable-length code words chosen to match the original source statistics, in this case the actual image or the version of its processed pixel values. This type of coding is usually reversible when viewing tables (LUTs). Huffman codes and an arithmetic coding technique are examples of an image code system that explores coding redundancy. [2].

### c) Psycho Visual Redundancy

Many psychological experiments with human vision show that the human eye does not respond to all incoming visual information with equal sensitivity; some information is more important than others. This type of redundancy is utilized by most current image encoding algorithms such as the discrete cosine transform(DCT), the core of the JPEG encoding standard. [3].

## II. IMAGE COMPRESSION MODEL

Figure 1 shows the basic square image compression diagram. The encoding component of the picture compression comprises of three distinct squares. The corresponding section[4] eliminates

the excess in the entomb pixels of this organization. [4].

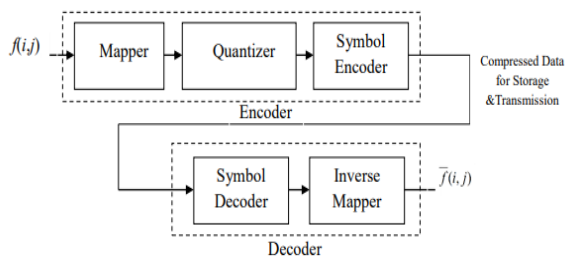


Fig 1. Image compression block diagram and decoder segment [4]

This programming period is reversible and the estimation of the details used to connect to the picture can be reduced easily. The quantization of lossless compression is irreversible and should be avoided. It reduces the loss of the psycho-visual image. Image encoder block encodes a quantified image into bits to be inserted or forwarded through a contact medium into a capacity gadget. [5]. This loop is reversible and is repeatedly coded. The coding can be fixed length coding or coding for variable length. The coding technique used commonly is a vector coding in which the quantization levels normally picked up are coded with lower bits, while the rest is coded in important pieces [6]. The compression section involves the image decoder and the mapper backwards. Image decoder discern the quantization levels from bits and these quantization levels are intended to get a comparative image. In the decoder field, the quantizer disappears backwards because it is irreversible. Between the information image and the compact image, the general information surplus is calculated (Re). At this point relative knowledge is likely that a number of parts required for the single image are b and compacted image b.

$$R_e = 1 - \frac{1}{CR} \dots 1.1$$

Where CR is one of the approximate limitations of the image compression procedure. CR is a compression rate. CR is the ratio of number of components needed for a single image to number of compact repeated images [7].

$$CR = \frac{b}{b'} \dots 1.2$$

The CR = 20 compression ratio reveals that 1 bit is adequate in the compacted image in uncompressed images for each 20 bits. If CR=20 does not reiterate relative information Re=0.95, that is to say 95% of the information is disproportionate at that point. Three cases arise:

Case 1: If  $b = b'$  at that point  $CR = 1$  and excess  $Re = 0$ , this demonstrates no repetition in the info image.

Case 2: If  $b \gg b'$  at that point  $CR \rightarrow \infty$  and repetition  $Re > 1$ , this shows excess in the information image.

Case 3: If  $b \ll b'$  and excess  $Re \rightarrow -\infty$ , this shows packed image require a larger number of pieces than the information image. Another presentation estimating boundary is bit rate (BR). For a dim scale image number of pieces required is 8 then BR is

$$BR = \frac{8}{CR} \text{ (bits/pixel (bpp))} \dots 1.3$$

BR = CR 0.4 bpp = 20. That means that 0.4 pieces/pixel are the quantity necessary to talk to the packaged image.

### 1.4 Image Compression and Reconstruction

The image compression norm will order three simple information redundancies[8].

- Spatial excess due to the link between the surrounding pixels.
- Spectral repeat since the shading sections are related.
- Psycho-visual excess due to individual visual framework features.

Since simple spatial and irresistible cases between pixes and shading parts are fundamental to each other, spatial and fantastic redundancies are given when the psycho-visual replay of certain spatial frequencies begins in the same way as a regular oeil is harsh[7]. The standard measurement of image compression is I to decrease the duplication in the image data, and (ii) to construct an image from the first frame, with error shown unrelated to the applications proposed[8]. The point of this data collection is to get a worthy visual image while retaining the basic details.

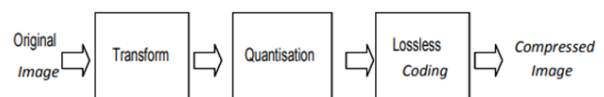


Fig2: Image compression system [8]

As seen in Figure 2, the question explored by image compression is anything but hard to describe. First the first digital image is usually converted into another region, in which any alteration is exceedingly unrelated[8]. The big image data is focussed on a smaller structure[8] in this sense. The blower removes the repetition in the altered image at that stage and saves it into a compacted record or data stream. The quantization block in the following stage reduces the exactness of the adjusted yield in

accordance with some scale of devotion. This step additionally lowers the knowledge image's psycho-visual excess[8]. Quantization is a reversible cycle that may be ignored if error-free or lost compression is necessary. The image coder makes a fixed or varying length code for the quantize output in the last step of the compression model, and directs the output as per the code. A variable-length code is often used to communicate about the knowledge collecting scheduled and quantum[8]. It assigns the shortest code words to yield estimates which most frequently occur and thereby reduces coding repeats. In reality, it is a reversible operation. The compression period is modified to create the restored image as seen in Figure 3. The image that you have retrieved may have been missing any data due to the compression, and the first image may have been mistake or twisting [9].

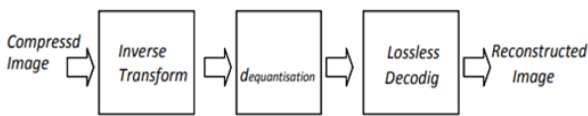


Fig 3. Image decompression System [9]

### III. VECTOR QUANTIZATION

A feasible loss compression technique [9] is a vector quantization that misappropriates all factual relationships within a supplied square to achieve RC. If X is a K-specific source vector (X1,...,XK), the Kdimensional VQ is a Q(X) power mapping X N into a M yield focus, each point connected to a Y1,Y2,...YM yielded an N-specific position [9]. The M yield vector, called a VQ codebook regularly and its associated non-covering parcels of RN meaning P1, P2... PM, the quantizer is determined by  $Q(X) = Y_i P_i$  THE FOR X,  $i=1, 2, \dots, M$ , according to the calculation of unnecessary mutilation. The theory of vector contortion, proposed by Shannon, offers an integral bound to the show of vector quantizers[9]. In the preparation of a VQ, the twist rate solution is to use Q(x) to minimise normal bending with the end objective that,

$$P_i = \{X : \|X - Y_i\| \leq \|X - Y_j\| \forall j \neq i\} \dots\dots\dots 1.4$$

VQ is a technique of square encoding where the information image is separated into small squares and in principle 4 pixels per square is converted into a vector, known as the preparation of the vector. These vectors are clustered into rafts which depend on the distance from euclidean, and the centre of each meeting is the codevector. Assortment of such codevectors structures the codebook. An ideal VQ would generate a size M codebook C for  $M < N$ , with minimum natural twisting[9]. The VQ encoder encodes the next codevector index in the codebook for each square. The codebook and code list structure the compacted stream and is therefore formed. The decoder retrieves its comparative codevector from the codebook by using the index code to recreate the

image. Figure 4 displays the schematic diagram of the VQ encoder [9]

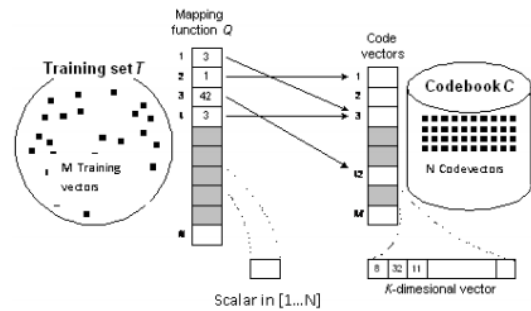


Fig 4 : VQ Encoder [10]

### IV. LITERATURE SURVEY

This proposal proposes a two-stage watermarking approach to validate the image by changing to upside vector quantification Archana Tiwari and Manisha Sharma et al. [2017]. During this measurement, two progressive steps are autonomously included in robust watermark and semi-fragile watermark. Strong watermarks and VQ strengthen the frame's protection by doubling the intended structure, whereas semi fragile watermarks help validate the image obtained. Shifting-sized watermarks are used in the cover image and are measured in terms of PSNR, weighted PSNRs and communication error. For identifiable documentation of an attack as useful or pernicious, an innovative technique is suggested. The findings demonstrate the strategy's ability to party assaults and find the modified area correctly. It is feasible to discern and settle on improvements which are extraordinarily large. The new schematic complies with previous calculations on indiscriminacy, criteria for structures for attacks, vigor, and alter exploration [10].

In this postulation, Akhand Pratap Singh, Dr. Anjali Potnis and Abhineet Kumar et al. [2016], the interest in information compression grows exponentially with the growth of current connectivity technologies. The paper includes an audit of the rules on compression, compression classes and various compression measurements. Image Compression is the resolution of optical image processing problems and the large digital image data measuring capacities. image compression integrates diverse uses, such as satellite, TV and other critical distance communications remote-detection. Satellite imagegraphs, clinical videos, documents and images need to be stored for images. For these types of uses, image compression is important. This paper aims to help pick genuinely excellent and renowned calculation for image compression [11].

Tooth et al. [2016] also adopted channel state information (CSI) rather than signal intensity for the

WiFi indoor system to boost channel prediction. The suggested measurement using a stalled discrete wavelet 7 shift (MDWT) has disintegrated and normalised the wavelet coefficients by using histogram equalisation. This calculation strengthened fingerprinted indoor localization. By reworking CSI with the other MDWT from the uniform coefficients, the striking highlights were removed [12].

The Electrocardiogram (ECG) analysis was initiated in Junior et al., [2016] providing separate series of details related to the present heart situation. One of the main problems in the electrocardiographic signal investigation is the QRS complex recognition. The RDWT uses Real-time QRS complex predictor for the repeated discrete wavelet transform. The equation uses both the wavelet and position coefficients of the wavelet. In light of QRS positions and wavelet coefficients, the computation was evaluated with an MIT-BIH Arrhythmia database which identifies buildings above 99.32% and can also be defined on P and T waves [13].

Duan et al., [2016] also implemented clinical, automatic and Surface electromyogram (SEMG). Extra hand action orders should be arranged to recover the ability of the myoelectric prosthetic hand. For extra hand action commands that can be clustered, the other SEMG sensors are used. It's not a joke to study the production-related example recognition equations in order to maximise the chance of myoelectric prosthetic side. Present examples of sEMG signals are checked using fractional identification examples and slow specific arrangements. To defeat the problem through the estimation of the relation between the Surface electromyogram DWT) and the wavelet neural network (WNN) [14].

The principle of image improvement was proposed by Lidong et al. (2016). It plays a critical function in the handling of images. Differentiation of CLAHE is a convincing measurement that helps improving the image of the results. Whatever the situation, it manages the separation and the improvement in noise. In order to deal with the issues described above, CLAHE names the procedures: discrete wavelet transforms (DWT). Three major developments were made in the new procedure: 1. First, DWT disintegrate the first image into recurrence segments for low 8 and high repetitions. Next, CLAHE's low-recurrent coefficients and do not restrict the noise increase by retaining the high-recurrence coefficients. This is because the extremely repeated section compares with informative details and includes more unique image noises. Finally, rework the image by using the new coefficients backward DWT [15].

Quan et al. (2016) presented signal and image preparation applications wavelet modifications. After the late date, attention has been given to graphics processing unit (GPU) in order to speed up computer-concentrated problems, and various provisions have been made to introduce a GPU-based discrete wavelet

transforms (DWT), but not to have the maximum effect on the GPU. The crossbreed approach to its presentation is eventually established through the use for example, of cutting-edge techniques for the GPU improvement of DWT, such as mutual memory, registers, twist reorganisation of directions and string-and guide level parallelism (TLP, ILP) [16].

## V. PROPOSED METHODOLOGY

The foundation of this compression method is this vector quantification and plan. CFA raw information is first screened with a low pass in the pre-processing phase. By inserting a partition block and following code mapping to 9-bit macros the vector pairs are quantified. JPEG-LS entropies these macros after reorganization. Closing and failure compression can be accomplished by changing the parameters of the preprocessor. For the Bavarian CFA results, this system is nearly loss-free as well as loss-free. In a frame, high-class reworked image graphs for diagnosis can be viewed in Nearly lossless fashion. Our capsule also constructs an ineffective mode which results in a smaller bit rate. If the capsule is in an area in which physicians are not interested in such items, a failing mode may be introduced to conserve electricity. Figure 5 indicates the scheme of the proposed system. In pre-selected mode, BAYA 8-bps is pre-processed and the two-pixel pair is vector quantified in 9-bit macros (near-lossless or lossy). The macros are translated to a compression engine JPEG-LS.

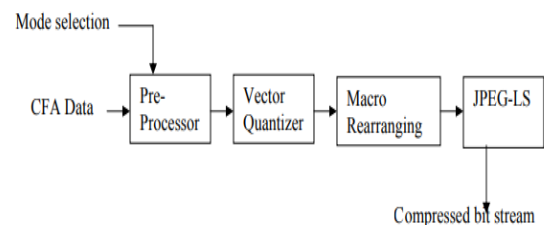


Fig 5. PVCC Process Block Diagram

The pre-processing phase is skipped in virtually lossless mode. Vector quantification is rendered using the same colour component on a pair of adjacent pixels. The vector measurement method can be represented in two parts: the divider block and the code map. During the block partition level, the redundancy of data is eliminated in an image. The code mapping is achieved to change the identity of the corresponding entropy encoding assigned to each block to maximise its compression efficiency. Thus a 2-D histogram is formed  $(x-y, x+y)$ , providing a pair of pixels has  $xy$   $(X, Y)$ . The histogram is not uniformly broken into 512 blocks. Therefore a block of 0 to 511 can be seen with an ID  $(x, y)$ . The laws of the partition are set as follows.

$$\text{BlockID} = \text{HeadID} + \frac{(x+y) - \text{BIAS}}{\text{STEP}}, \quad (x-y) \in \text{interval} \quad \dots 1.5$$

Table 1 lists the necessary interval scope, HeadID, BIAS and method. 1. The block division can be extracted from the table below and Equation 1.5, that the absolute value of the partition (x-y) is perfectly zero in the histogram region. The lower the gap, the higher the block is between a couple of pixels. This type of partition is explained by both the human visual system (HVS) and mathematical studies. A simple HVS property reveals an error on the edges of the unit that is less noticeable.

**Table 1: The intervals used in block partitions and their respective parameters**

Interval	HeadID	BIAS	STEPS
[-1,1]	0	0	4
[2,11]/[-11,-2]	128/170	2	12
[12,21]/[-21,-12]	212/252	12	12
[22,31]/[-31,-22]	292/330	22	12
[32,47]/[-47,-32]	368/397	32	15
[48,63]/[-63,-48]	426/453	48	15
[64,111]/[-111,-64]	480/487	64	54
[112,159]/[-159,-112]	494/499	12	54
[160,207]/[-207,-160]	504/507	160	54
[208,255]/[-255,-208]	510/511	208	95

Broad pixels (x-y) indicate the 2-D edge regions are represented. In regions where (x-Y) is small, the rules of block partition will reduce perceptible irrelevance by fine tuning. Statistical findings reveal that the area from (x-y) through[-31,31] covers more than 80 percent of macros. The possibility that macros will collapse in this region is such that we call it "heat." which is finely segregated into blocks by a rule on hotfield partitioning. This reduces the unavoidable vector quantification error to a minimal.

The appropriate BlockId code 0 to 511 will be obtained by (x,y) vector after the partition block (i.e. 9 bits). The outcome has a rate of 4.5 bpp. This method of compression uses an encoder to encrypt the macros. JPEG-LS encodes many existing lossless compression methods. The JPEG-LS algorithm is based on DPCM and existing projection values are based on its neighbouring macros. This revises the code allocated to each block by equations 1.5 to improve the value of adjacent macros to properly use JPEG-LS compression capability. The following blocks will obtain estimated BlockID values after code Mapping from 0 to 367 blocks in a hot zone (region (x-y)[-31,31]. BlockID is BlockID mapped. BlockID [32,63] except for blocks [x-y] and BlockID blocks [64,255], except for blocks [23]. In comparison, there were also blocks [-63,-32] (x-y) and [- 255,-64]. Until sending to

JPEG-LS for compilation, vector quantization macros may be stored as fresh images. In order to convert these macros into a different G/B/R pattern, the following JPEG-LS algorithm improves compressive efficiency and applies the makro arrangement package. The resolution of Figure 6 in 8 to 4 bits is translated in Figure 7 in Resolution 8 to 2 and 9 bits after the quantification of vectors and macro structure. The G12 is the product of vector quantization (G1,G2).

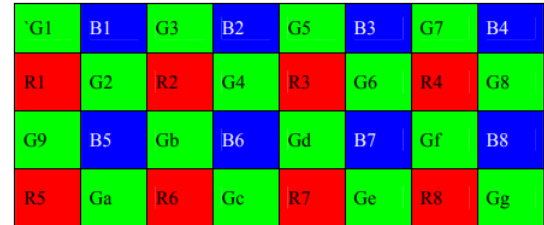


**Fig 6: Color Pattern of Bayer CFA Data**



**Fig 7: Separate G/B/R pattern rearranged macros**

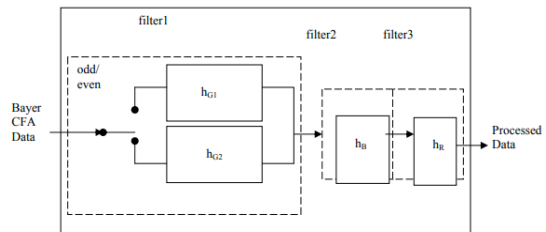


**Fig 8. PVCC Method Preprocessor Architecture**

The Bayer CFA data is sent to the pre-processing system when loss mode is chosen. There are three serial low-pass philtres for filtering with the elements G, B and R in the preprocessor. The architecture of the preprocessor can be seen in Figure 8 Filter1 for G in the following pulse duplication:

$$h_{G1} = \frac{1}{4} \begin{bmatrix} 0 & 1 & 0 & 1 & 0 \\ 1 & 0 & 1 & 0 & 0 \\ 0 & 0 & 0 & 0 & 0 \end{bmatrix}$$

$$h_{G2} = \frac{1}{4} \begin{bmatrix} 1 & 0 & 1 & 0 & 0 & 0 & 0 \\ 0 & 1 & 0 & 1 & 0 & 0 & 0 \\ 0 & 0 & 0 & 0 & 0 & 0 & 0 \end{bmatrix}$$

The pulse response for B and R components of filter2 and filter3 is:

$$h_{B/R} = \frac{1}{4} \begin{bmatrix} 1 & 1 & 0 \\ 1 & 1 & 0 \\ 0 & 0 & 0 \end{bmatrix}$$

By pre-processing, the importance of nearby pixels will be increased and other macros in the hot zone will fall. By code mapping the assignment of BlockID in a hot region would better match JPEG-LS compression, with a higher compression rate. Subsequently, vector measures, macro arrangements, and JPEG-LS compression were carried out following pre-processing of the collected Bayer material. In the preprocessing stage the image is overly smooth. This triggers a lack of peak signal to noise ratio (PSNR). In almost lossless mode the rate found in this device is approximately 4bpp, which is similar to the LCBF without loss..

### VI. RESULT ANALYSIS

The output of EMAC and many other SSACI compression algorithms including JPEG-LS, JPEG 2000 and Lossless Color Compression Images can be shown in Bit Rate Table 2. The predicted EMAC in Table 2 is less than the other bitrate (bpp) technique (JPEGLS, JPEG2000, and LCMI). By mounting the character for all 24 images, the best bit rate values are displayed individually. A decrease of 0.03bps for LCMI, 0.11bpp for JPEG2, and 0.95bpp for JPEG LS has been found in the EMAC algorithm indicated.

The JPEG-LS, JPEG2000, LCMI and EMAC comparative bitrate graph for the 24 kodak Table 3 compares PLCM to numerous other SSACI compression algorithms including JPEG-LS, JPEG2000, and Bayer Color Filter Series loss free image compression (LCBF). The table indicates that PLCM is the lowest bit rate for other methods in comparison with (bpp). A reduction of 0.6bpp (14%) on JPEG2000, 0.94bpp (23 percent) on JPEG2, and 1,78bpp (43%) on JPEG-LS was noted in the PLCM algorithm proposed. A graph demonstrating 24 modes of Kodak in Figure 10 is seen with JPEG-LS, JPEG 2000, LCBF and PLCM. This graph is shown, JPEG2000, LCMI, EMAC, LCBF and PLCM display average bit rate charts in Figure 11. Figure 11 screens. This figure demonstrates that the PLCM solution proposed overcomes all SSACI compression for the lossless SSACI compression as specified in the Bit rate.

**Table 2: Different lossless SSACI coding with EMAC contrast of bit rate (bpp)**

Image/ method	JPEG-LS	JPEG2000	LCMI	EMAC
1	6.4	5.82	5.82	<b>5.81</b>
2	6.79	5.13	4.77	<b>4.76</b>
3	5.88	4.21	3.97	<b>3.97</b>
4	6.68	4.95	4.75	<b>4.75</b>
5	6.47	5.95	5.86	<b>5.75</b>
6	5.87	5.2	5.14	<b>5.12</b>
7	5.97	4.48	4.3	<b>4.27</b>
8	6.29	<b>5.90</b>	5.95	5.92
9	5.07	4.39	4.36	<b>4.34</b>
10	5.39	4.56	4.52	<b>4.42</b>
11	5.37	4.97	4.97	<b>4.95</b>
12	4.63	4.49	4.41	<b>4.4</b>
13	6.75	<b>6.37</b>	6.42	6.39
14	6.29	5.56	5.51	<b>5.51</b>
15	6.32	4.68	4.48	<b>4.48</b>
16	5.29	4.55	4.56	<b>4.54</b>
17	4.96	4.54	4.55	<b>4.54</b>
18	6.18	5.58	5.54	<b>5.51</b>
19	5.4	4.89	4.95	<b>4.74</b>
20	4.32	4.03	4.19	<b>4.17</b>
21	5.47	5.04	5	<b>4.98</b>
22	6.19	5.21	5.13	<b>5.11</b>
23	6.83	4.53	4.04	<b>4.04</b>
24	5.72	5.22	5.26	<b>5.1</b>
Average	5.85	5.01	4.93	<b>4.90</b>

**Table 3: Comparison of Bit Rate (bpp) of Different Lossless SSACI Coding with PLCM**

Image/ method	JPEG-LS	JPEG2000	LCBF	PLCM
1.	6.4	5.82	5.48	<b>4.88</b>
2.	6.79	5.13	4.33	<b>3.89</b>
3.	5.88	4.21	3.75	<b>3.40</b>
4.	6.68	4.95	4.38	<b>4.26</b>
5.	6.47	5.95	5.40	<b>3.90</b>
6.	5.87	5.2	<b>4.88</b>	4.96
7.	5.97	4.48	<b>3.96</b>	4.04
8.	6.29	5.9	5.57	<b>3.72</b>
9.	5.07	4.39	4.19	<b>3.71</b>
10.	5.39	4.56	4.23	<b>3.82</b>
11.	5.37	4.97	4.68	<b>3.90</b>
12.	4.63	4.49	<b>4.09</b>	4.30
13.	6.75	6.37	6.14	<b>4.00</b>
14.	6.29	5.56	5.17	<b>3.85</b>
15.	6.32	4.68	4.10	<b>4.02</b>
16.	5.29	4.55	4.37	<b>4.30</b>
17.	4.96	4.54	4.56	<b>4.46</b>
18.	6.18	5.58	5.56	<b>4.24</b>
19.	5.4	4.89	4.22	<b>3.93</b>
20.	4.32	4.03	4.24	<b>3.70</b>
21.	5.47	5.04	5.71	<b>4.47</b>
22.	6.19	5.21	4.11	<b>3.83</b>
23.	6.83	4.53	3.98	<b>3.69</b>
24.	5.72	5.22	4.97	<b>4.49</b>
Average	5.85	5.01	4.67	<b>4.07</b>

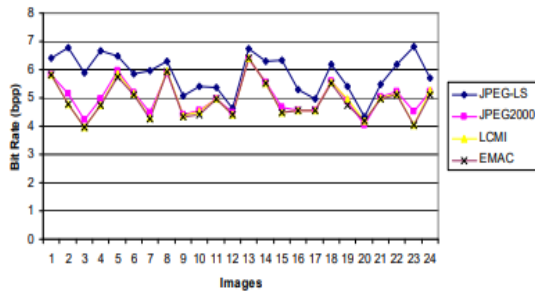


Fig 9: Comparison with EMAC bit rate of separate SSACI lossless codes (bpp)

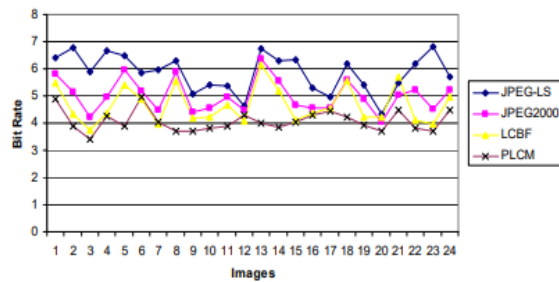


Fig 10: Bit Rate (bpp) Comparison of Different Lossless SSACI Coding with PLCM

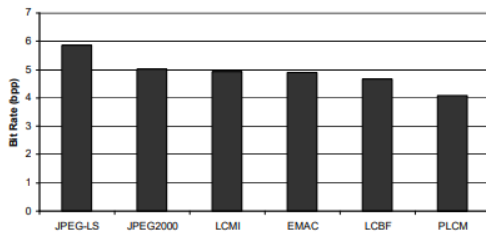


Fig 11: Comparison of different Lossless SSACI codings with EMAC and PLCM Average bit rates (bpp)

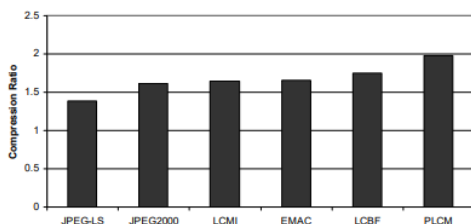


Fig 12: Comparison of various loose-free coding for EMAC and PLCM Average compression ratio

## VII. CONCLUSION

The main objective of the analysis was to improve the Bavarian movement to address key issues by building a new class of single sensor array image camera techniques, namely not to forecast the use of spatial and spectral similarities, inefficient border and smooth prediction identification, low resolution (PSNR), low bits and improved computing co-operation. Four

various types of algorithms have been developed and implemented: lossless domain coding, loose space domain and loss of space domain coding. We developed and adopted the following four algorithms. A single algorithm for Lossless SSACI frequency domain coding is the first type. The second category contains an algorithm in the Lossless SSACI coding space area, Lossless Compression of Mosaic images (PLCM), and two prediction-based mosaic compression (PLCM) algorithms. The third category consists of two PLCMs. The Successful Lossless Encoding of mosaic images with the Adaptive Background-Based Coding was employed to remove statistical redundancies in spectral and space. EMAC proposed a coding to classify the edge of the transformed image for the adaptive edge sensing (sharp and smooth region). The experimental results suggest that EMAC is superior to advanced technologies and the latest approaches to compression in the SSACI frequency domain (JPEG-LS, JPEG2000). Centered on estimation, the Lossless Encoding of mosaic images utilizes a powerful backdrop technique for detection of surrounding pixels. In order to prevent colour redundancies, a pixel approximation was proposed by an adaptive colour differential system, classifying the edges as sharp, 'average' or weak and by using the assessment to rectify the prediction value. EMAC has so far met all the SSACI lossless Bit Rate compression reports by experience performance. Tests prove. The Lossy encoding of mosaic images in the frequency domain indicated a classified vector quantization (CVQ). In normal vector quantization, the problem of edge erosion improved. Experimental results indicate that LCMF beats existing state of the art approaches visually as as regards a peak signal to noise ratio (PSNR). Effective use of discrete transform cosine characteristics is cost-effective mosaic imaging coding (CECM). This methodology suggested the encryption by entropy coding of the minimal DCT coefficient to minimise computational complexities. This methodology Experimental trials indicate that CECM performs at higher concentrations than the more sophisticated methods. Vector-based quantizing processing, the near-lossless Mosaic Image Compression (VNMC), suggested vector quantified pixels in 9-bit macros by incorporating the block partition. After rearranging these macros became compressed JPEG-LS. The experimental results support the good compression rate and image quality of the compression system proposed.

## REFERENCES

- 1) Uli Grasmann and Risto Miikkulainen (2005). Effective Image Compression using Evolved Wavelets, ACM, pp. 1961-1968.
- 2) Ming Yang and Nikolaos Bourbakis (2005). An Overview of Lossless Digital Image Compression Techniques, IEEE, pp. 1099-1102.

- 3) Mohammad Kabir Hossain, Shams MImam, Khondker Shajadul Hasan and William Perrizo (2008). A Lossless Image Compression Technique Using Generic Peano Pattern Mask Tree, IEEE, pp. 317-322.
- 4) Tzong Jer Chen and Keh-Shih Chuang (2010). A Pseudo Lossless Image Compression Method, IEEE, pp. 610-615.
- 5) Jau-Ji Shen and Hsiu-Chuan Huang (2010). An Adaptive Image Compression Method Based on Vector Quantization, IEEE, pp. 377-381.
- 6) Suresh Yerva, Smita Nair and Krishnan Kutty (2011). Lossless Image Compression based on Data Folding, IEEE, pp. 999-1004.
- 7) Firas A. Jassim and Hind E. Qassim (2012). Five Modulus Method for Image Compression, II SIPIJ Vol.3, No.5, pp. 19-28.
- 8) Mridul Kumar Mathur, Seema Loonker and Dr. Dheeraj Saxena (2012). Lossless Huffman Coding Technique For Image Compression And Reconstruction Using Binary Trees, IJCTA, pp. 76-79.
- 9) V.K Padmaja and Dr. B. Chandrasekhar (2012). Literature Review of Image Compression Algorithm, IJSER, Volume 3, pp. 1-6.
- 10) Archana Tiwari and Manisha Sharma (2017). "An Image Authentication Algorithm Using Combined Approach of Watermarking and Vector Quantization" J. Intell. Syst.
- 11) Akhand Pratap Singh, Dr. Anjali Potnis, Abhineet Kumar (2016). "A REVIEW ON LATEST TECHNIQUES OF IMAGE COMPRESSION" International Research Journal of Engineering and Technology (IRJET) e-ISSN: 2395 -0056 Volume: 03 Issue: 07.
- 12) Fang (2016). "Texture segmentation using wavelet transform", Pattern Recognition Letters, Vol.24, No.16, pp.3197-3203.
- 13) Junior (2016). "Simultaneous algebraic reconstruction technique (SART): a superior implementation of the art algorithm", Ultrasonic Imaging, Vol. 6, No. 1, pp. 81–94.
- 14) Duan (2016). "An efficient single image super resolution algorithm based on wavelet transforms", IEEE Machine Vision and Image Processing (MVIP), Iranian Conference, pp. 111-114.
- 15) Lidong (2016). "CT Reconstruction from Parallel and Fan-Beam Projections by a 2-D Discrete Radon Transform", IEEE TRANSACTIONS ON IMAGE PROCESSING, Vol.21, No.2, p.733.
- 16) Quan (2016). "3D ROI Image Reconstruction from Truncated Computed Tomography", IEEE Transactions on Medical Imaging, Vol.11, No. 9.

---

### Corresponding Author

**Mr. Surya Pratap Singh\***

Research Scholar, SRK University, Bhopal